A Vortex Sheet Method for Calculating Separated Two-Dimensional Flows

M. Ribaut*
Brown Boveri Ltd., Baden, Switzerland

A mixed boundary condition problem for the time-averaged separated flow of a compressible and viscous fluid at high Reynolds number is formulated and solved by means of vortex and source integral equations involving vorticity diffusion. Application of the method to the flow past a flat plate and a blunt trailing-edge section has shown that the extension and underpressure of the calculated wakes directly depend on the amount of vorticity diffusion and dissipation occurring in the flow. Computed velocity distributions and wake underpressures are compared with the experiment.

Nomenclature

a	= sound velocity
c	= fluid velocity
c_∞	= freestream velocity
C_p	= pressure coefficient
$\bar{C}_p$	= underpressure coefficient
d	= trailing-edge thickness upstream of taper
g	= vorticity distribution function
H	= channel height
$h,k,k_{1,2,3}$	= shape parameters of vorticity distribution
$K,K_{1,2}$	= geometrical kernels
L	= plate length or trailing-edge thickness
n	= normal to the wall or the vortex sheet centerline
q	= source density (divergence of c)
$\bar{q}$	= strength of a source layer ($q\cdot\delta$)
Q	= vortex separation number
s	= distance on the profile and the vortex sheet centerlines
t	= diffusion parameter
x,y,z	= Cartesian coordinates
X,Z	= profile parameters
α	= angle between vortex sheet centerline and freestream direction
γ	= vortex density (curl of c)
$\bar{\gamma}$	= strength of a vortex layer ($\gamma\cdot\delta$)
$\bar{\gamma}_D$	= vortex strength leaving the solid surface
δ	= thickness of a vortex or source layer
$\partial\Omega$	= set of the points on the active boundary surface and the vortex sheet centerlines
λ_F	= vorticity diffusion coefficient
λ_S	= vorticity dissipation coefficient
θ	= angle between plate surface and freestream direction
Ω	= set of the points wetted by the fluid
Subscripts	
$0,1$	= wall, wake part of a boundary layer
D	= relative to the separation point
e	= outside of the wake
s	= current point of the integrals
x,y	= in x,y direction

Introduction

IN recent years the calculation of separated flows by means of vortex methods has undergone considerable development. Most of these methods use time-dependent techniques tracking in a Lagrangian reference frame the vorticity generated at the boundary surface and dispersing into the flow.[1] The potential ability of such methods to simulate flows at high Reynolds numbers is certainly considerable, also the solutions are rather sensitive to the choice of differencing schemes or time steps. In particular, the numerical scatter of the vortices in the regions of low convection velocity makes it difficult to appreciate the real influence of the viscous vorticity diffusion on the shape and extension of the wake. Other methods calculate a steady-state solution with free vortex lines,[2] displaced streamlines,[3] or apparent body shapes[4] and try to find a streamline of the inviscid fluid flow producing the pressure distribution of the real flow. On the free part of this streamline, the inverse boundary conditions can be satisfied either by integration of the velocity vector,[2] conformal mapping,[4,5] or perturbation methods.[3,6] If the pressure is constant on the free streamline, the resulting wake has an infinite extension and no underpressure (e.g., Chaplygin-Lavrentiev flows[5]). The problem is therefore to predict the pressure difference between the separation point and the end of the wake and to find the wake shape or to assume the wake shape and to find the pressure difference. The contribution of the present study is to show that this problem can be avoided by introducing vorticity diffusion or dissipation in the vortex line model and to demonstrate that the extension and underpressure of the wake are essentially determined by the amount of viscous diffusion and dissipation of the vorticity leaving the solid surface.

Boundary Condition Problem

At first we consider the separated jet flow of an inviscid fluid past a two-dimensional profile (Fig. 1a). On the free streamlines the solution is discontinuous and determined by inverse boundary conditions. The resulting mixed boundary condition problem can be solved by the conformal mapping technique[5] or, with more generality, by means of a vorticity distribution on the boundary surface and the free streamlines.[6] Strength or location of this vorticity are obtained by formulating one or two of the following boundary conditions

$$n\cdot c[x,y,\bar{\gamma}(x_s,y_s)]=0 \qquad |n|=1 \tag{1a}$$

$$n\times c[x,y,\bar{\gamma}(x_s,y_s)]=-\tfrac{1}{2}\bar{\gamma}(x,y) \tag{1b}$$

in discrete points $P(x,y)$ of the boundary surface and the free streamlines. On the active part of the solid boundary the position of the vorticity $\bar{\gamma}(x_s,y_s)$ is known and its strength is considered as explicit unknown. On the free streamlines the inverse is true: the vorticity has a constant strength $\bar{\gamma}(B)$ or $\bar{\gamma}(D)$ and its ordinate y_s may be considered as explicit unknown. Applying a Taylor development to the left-hand

Presented as Paper 82-1030 at the AIAA/ASME Third Joint Thermophysics, Fluids, Plasma and Heat Transfer Conference, St. Louis, Mo., June 7-11, 1982; submitted June 17, 1982; revision received Nov. 16, 1982.

*Scientific Assistant, Turbocharger Department.

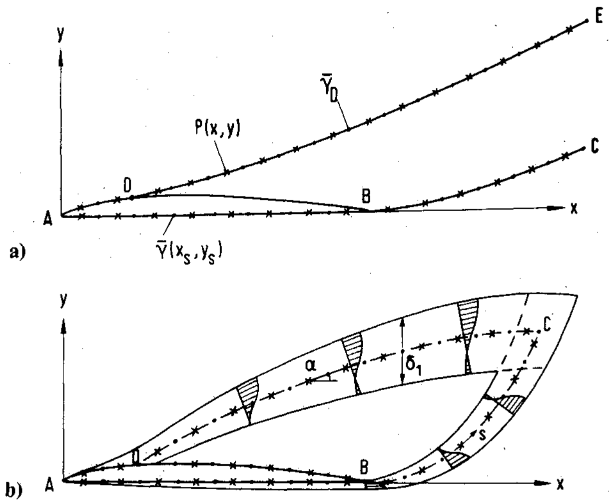

Fig. 1 Flow models for the inviscid and viscous fluid flow.

side of Eq. (1a), we can write[6]

$$\left[n(x,y^*)+\frac{\partial n}{\partial y}\Delta y\right]\cdot\int_{\partial\Omega}\left[K(x,y^*,x_s,y_s^*)\bar\gamma + \left(\frac{\partial K}{\partial y}\Delta y+\frac{\partial K}{\partial y_s}\Delta y_s\right)\bar\gamma^*\right]\mathrm{d}s=F^*(x,y) \tag{2}$$

where Δy is the relative position of the free vortex lines and F represents the unperturbed flow as well as the inhomogeneous part of the local conditions ($\nabla\cdot c\neq 0$). Assuming initial values for $\bar\gamma^*$, y^*, and F^*, which are introduced iteratively, the linearized equation system (2) provides the vorticity distribution and a new position of the free vortex lines. The converged solution will be unique if, in the first place, the separation points of the flow are determined and, in the second place, the following steadiness condition is satisfied:

$$\bar\gamma(B)+\bar\gamma(D)=0 \tag{3}$$

If we consider now the separated flow of a viscous fluid at high Reynolds number (Fig. 1b), the thin free vortex sheets may still represent a zone of insufficient continuity for a numerical computation proceeding with finite integration steps. It is therefore probable that the solution to the mixed boundary condition problem described above is also appropriate to the calculation of the viscous fluid flow at high Reynolds numbers. The appearance of viscosity in the fluid has two consequences for the vortex integral equation (2). First, the no-slip condition at the boundary surface implies a new definition of the vortex strength,

$$\bar\gamma=\int_0^{\delta}\gamma(n)\,\mathrm{d}n \tag{4}$$

Thus, the homogeneous boundary conditions of the viscous fluid flow can still be satisfied with a vorticity distribution associated to each point of the boundary surface.[7] Second, the distribution of the vorticity in the direction normal to the boundary surface, which results from viscous diffusion, must be defined and introduced as a priori knowledge in the calculation. This will be the subject of the next section.

Vorticity Diffusion

The dual structure of a turbulent boundary layer can be accounted for by considering a wall region of thickness δ_0 bearing the vortex strength $\bar\gamma_0$ and a wake region bearing the vortex strength $\bar\gamma_1$,

$$\bar\gamma_0=\int_0^{\delta_0}\gamma_0(n)\,\mathrm{d}n \tag{5a}$$

$$\bar\gamma_1=\int_{\delta_0}^{\delta}\gamma_1(n)\,\mathrm{d}n \tag{5b}$$

Thus, a first broad distribution of the vorticity can be determined by means of a boundary-layer or wake thickness and two profile parameters,

$$X=\delta_0/\delta \tag{6a}$$

$$Z=\bar\gamma_0/\bar\gamma \tag{6b}$$

Inside of the two regions considered, the vorticity is defined by a distribution function involving a certain number of shape parameters,

$$\gamma_0=(\bar\gamma_0/\delta_0)\,g_0(n,h,\ldots) \tag{7a}$$

$$\gamma_1=(\bar\gamma_1/\delta_1)\,g_1(n,k,\ldots) \tag{7b}$$

Making use of Coles's law of the wake,[8] the following functions may be considered:

$$g_0=k_1+k_2\left(\frac{n}{\delta_0}\right)^{h-1} \tag{8a}$$

$$g_1=k\left(1-\frac{n-\delta_0}{\delta_1}\right)+k_3\sin\left(\frac{n-\delta_0}{\delta_1}\pi\right) \tag{8b}$$

to which correspond the "viscous" horizontal velocity distributions

$$c_0=\bar\gamma_0\left[k_1\frac{n}{\delta_0}+k_2\frac{1}{h}\left(\frac{n}{\delta_0}\right)^{h}\right] \tag{9a}$$

$$c_1=\bar\gamma_0+\bar\gamma_1\left\{k\frac{n-\delta_0}{\delta_1}\left(1-\frac{1}{2}\frac{n-\delta_0}{\delta_1}\right)+k_3\frac{1}{\pi}\left[1-\cos\left(\frac{n-\delta_0}{\delta_1}\pi\right)\right]\right\} \tag{9b}$$

and, for a continuous vorticity distribution, the closure conditions

$$k_1=\frac{h}{h-1}\left(1-\frac{k}{h}\frac{X}{1-X}\frac{1-Z}{Z}\right) \tag{10a}$$

$$k_2=-\frac{h}{h-1}\left(1-k\frac{X}{1-X}\frac{1-Z}{Z}\right) \tag{10b}$$

$$k_3=(\pi/2)(1-½k) \tag{10c}$$

The shape parameters h and k are a measure of the relative magnitude of the vorticity near the wall and in the interaction zone of the two layers. In general, they will depend little on the profile parameters X and Z. For a turbulent boundary layer the thickness δ_0 and the linear term of g_1 are small, so that we may write

$$\bar\gamma=Z\bar\gamma+(1-Z)\bar\gamma\frac{\pi}{2\delta}\int_0^{\delta}\sin\left(\frac{n}{\delta}\pi\right)\mathrm{d}n \tag{11}$$

the part $Z\bar\gamma$ of the vorticity being concentrated on the wall. The values of Z and δ can be obtained from a boundary-layer calculation. Downstream of the separation point ($Z=0$), the thickness of the vortex sheet can be approximated by the following expression[9]:

$$\delta=\delta_D+\lambda_F \frac{L}{2}\left(\frac{s-s_D}{0.5L}\right)^t \tag{12}$$

where the exponent takes into account the laminar ($t=0.5$) or turbulent ($t=1$) character of the flow and L is a characteristic length of the solid surface.

The assumption of free vortex sheets having a constant strength downstream of the separation point could be too restrictive in the case of a real fluid flow. If the vortices leaving a solid surface behave like those produced by turbulence[10] and degenerate into vortices of reduced size, some dissipation of the vorticity must occur at the end of the cascade. Thus, we assume

$$\bar{\gamma}=\bar{\gamma}_D\left(1-\lambda_S \frac{s-s_D}{0.5L}\right) \tag{13}$$

To insure the steady state with this vorticity distribution it is necessary to apply Eq. (3) to the intersection of the two vortex sheets leaving the solid surface (Fig. 1b),

$$\bar{\gamma}(B)\left(1-\lambda_S\frac{s(C)-s(B)}{0.5L}\right) + \bar{\gamma}(D)\left(1-\lambda_S\frac{s(C)-s(D)}{0.5L}\right)=0 \tag{14}$$

From the mathematical point of view, the introduction of a vorticity dissipation is unproblematic, since it is always possible to multiply a curl vector by a scalar, the gradient of which is normal to this vector, to obtain a new solenoidal vorticity field. However, the latter will not satisfy to the principle of vorticity conservation implied by the vorticity transport equation.

Calculation of the Velocity Field

The velocity field of any compressible and viscous fluid flow can be represented by a linear integral function involving its divergence and curl as well as the integrated forms $\bar{q}$ and $\bar{\gamma}$ of these operators, which arise from boundary conditions or other restrictions (e.g., shocks) and account for the discontinuities of the flowfield. The velocity components of the two-dimensional flow illustrated in Fig. 1 can be written as[6]

$$c_x(x,y)=\frac{1}{2\pi}\int_{\partial\Omega} K_1\bar{\gamma}\mathrm{d}s+\frac{1}{2\pi}\int_\Omega K_2 q\,\mathrm{d}x_s\mathrm{d}y_s+c_{\infty x} \tag{15a}$$

$$c_y(x,y)=-\frac{1}{2\pi}\int_{\partial\Omega} K_2\bar{\gamma}\mathrm{d}s+\frac{1}{2\pi}\int_\Omega K_1 q\,\mathrm{d}x_s\mathrm{d}y_s+c_{\infty y} \tag{15b}$$

with

$$K_1=\frac{y-y_s}{(x-x_s)^2+(y-y_s)^2} \tag{16a}$$

$$K_2=\frac{x-x_s}{(x-x_s)^2+(y-y_s)^2} \tag{16b}$$

The last term on the right-hand side of Eqs. (15) represents the unperturbed flow, whereas the second integral takes into account the compressibility of the fluid and the eventual three-dimensional character of the flow,

$$q=\frac{c^2}{a^2}\nabla c-c_x\frac{1}{H}\frac{\partial H(x)}{\partial x} \tag{17}$$

Making use of Eqs. (15) and (16), the boundary condition [Eq. (2)] becomes

$$\frac{1}{2\pi}\int_{\partial\Omega}\left[K\bar{\gamma}+\left(\frac{\partial K}{\partial y}\Delta y+\frac{\partial K}{\partial\alpha}\frac{\partial\alpha}{\partial y}\Delta y+\frac{\partial K}{\partial y_s}\Delta y_s\right)\bar{\gamma}^*\right]\mathrm{d}s$$
$$=-\frac{1}{2\pi}\int_\Omega[K_2\sin\alpha-K_1\cos\alpha]\,q^*\mathrm{d}x_s\mathrm{d}y_s$$
$$-c_{\infty x}\sin\alpha+c_{\infty y}\cos\alpha \tag{18}$$

with

$$K=K_1\sin\alpha+K_2\cos\alpha \tag{19}$$

If Eq. (18) is formulated on the solid boundary surface, the second and third terms on the left-hand side drop out. Similarly, the fourth term will be omitted if the current point of the integral is situated on this surface.

The calculation of the velocity field can then be summarized as follows. In a first step Eq. (18) is formulated at discrete points of the boundary surface by considering only the first term on the left-hand side and the two last terms on the right-hand side. Together with the steady condition of Eq. (3), this equation system provides a first distribution of the vorticity. The velocity field is then calculated, either with Eqs. (15) or with the faster finite difference method,[7] and first values of the divergence determined with Eq. (17). Information about the separation points is obtained from a boundary-layer calculation and a first shape of the centerlines of the free vortex sheets assumed (e.g., streamlines of the unperturbed flow). In the following steps, all calculations are repeated but formulating Eq. (18) and involving the normal vorticity distributions [Eqs. (11-13)] on the solid boundary and the vortex sheet centerlines. Here, the steady condition of Eq. (14) will be used. After convergence of the solution, the vorticity associated to each point of the boundary surface, the vorticity flowing off within the free vortex sheets as well as their position in the flowfield are known.

Separated Plate Flow

The present method was applied to the flow past a flat plate at angles of attack between 15 and 90 deg. Under these flow conditions, the development of the boundary layer on the windward side of the plate is small. It was therefore assumed that the vorticity associated with this side is concentrated on the boundary surface. A first set of calculations was carried out for the inviscid fluid flow. Equation (18) was formulated

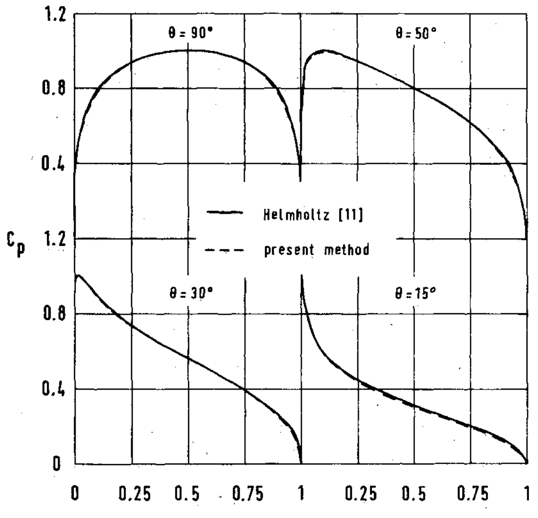

Fig. 2 Prediction accuracy for the inviscid fluid flow.

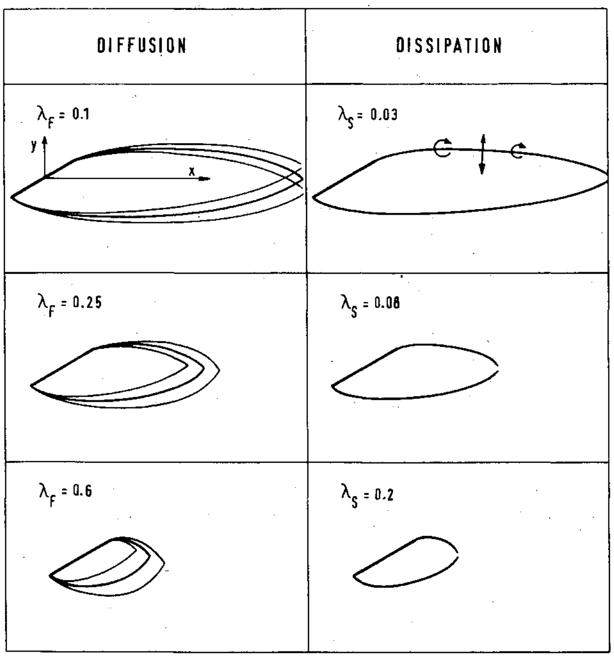

Fig. 3 Influence of vorticity diffusion or dissipation on wake extension.

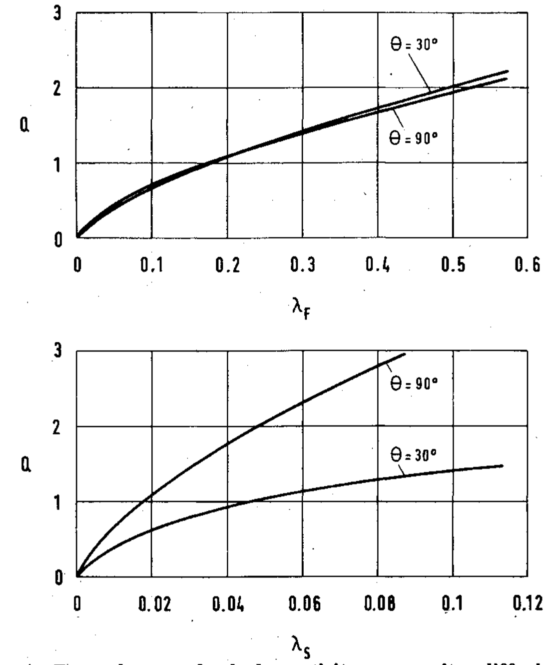

Fig. 4 Dependence of shed vorticity upon its diffusion or dissipation.

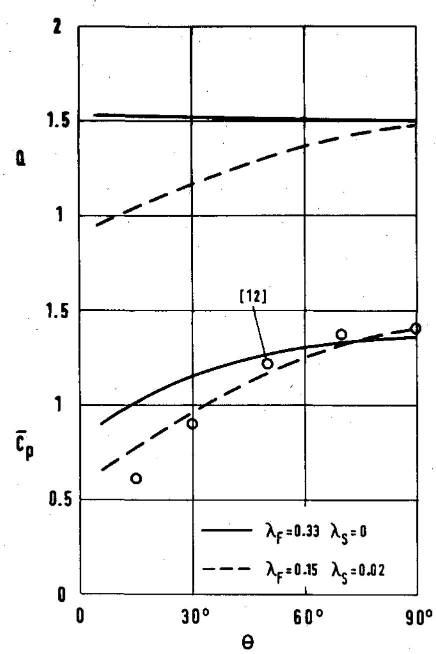

Fig. 5 Predicted vortex separation number and underpressure.

at the midpoint of 20 equidistant intervals on the plate surface and 125 intervals on each vortex line leaving the plate edges. These vortex line segments were extended linearly to a distance about 300 times the plate length in order to account for the infinite extension of the wake. Convergence of the solution was achieved within 15 iterations and after a calculation time of 20 min using an IBM 370-168. The results are compared in Fig. 2 with the exact solutions of the jet flow theory.[11] Details of the calculation can be found in Ref. 6.

To investigate the influence of the vorticity diffusion or dissipation on the extension and underpressure of the wake, a number of calculations with different values of the diffusion and dissipation coefficients were performed for the turbulent flow past a plate inclined at 30 deg. The results are shown in Fig. 3 and demonstrate that the finite configuration of the wake is directly determined by the amount of vorticity diffusion or dissipation occurring in the flow. The mechanism of this action is purely kinematical and is illustrated at the top of Fig. 3. It will be seen that any decrease of the vorticity in the downstream direction, resulting either from diffusion or dissipation, moves the two vortex sheets toward the inside of the wake, thus reducing its extension and increasing the curvature of the streamlines at the plate ends and therefore the amount of vorticity leaving the plate. This latter may be defined by the vortex separation number

$$Q = (\bar{\gamma}_D / c_\infty)^2 - 1 \tag{20}$$

the dependence of which on the diffusion and dissipation coefficients defined by Eqs. (12) and (13) is shown in Fig. 4. Let us observe that the plate inclination has practically no effect on the influence of the vorticity diffusion on the vortex separation number, whereas it considerably increases the influence of the vorticity dissipation. This is confirmed by the vortex separation numbers and underpressure coefficients plotted in Fig. 5 against the plate inclination. The underpressure coefficient was obtained from the computed velocity at the outside of the wake, assuming an isentropic variation of the pressure in the mainstream,

$$\bar{C}_p = \frac{1}{L\cos\theta} \int_0^{L\cos\theta} \left[\left(\frac{c_e}{c_\infty} \right)^2 - 1 \right] \mathrm{d}x \tag{21}$$

It may be observed that the difference between the vortex separation number and the underpressure coefficient decreases with the plate inclination and reduces practically to zero for the plate normal to the wind. The explanation of this situation lies in the existence of a reversal flow in the wake, which reduces the mainstream velocity and therefore the underpressure. An illustration of this wake flow is given in Fig. 6 for the laminar and turbulent flow without vorticity dissipation. It can be observed that the amount of reversal flow is essentially determined by the relative proximity of the leading-edge vortex sheet to the plate. Indeed, depending on this proximity, the vorticity of this sheet induces on the upstream half of the plate more or less normal velocity adding to the one of the unperturbed flow, thus producing an increase of the whole plate vorticity (Fig. 7) which has to annul this velocity. As a consequence of this kinematical mechanism, as the plate inclination decreases and the vortex sheet thickens, the more the vorticity leaving the plate and the reversal flow in the wake increase. The velocity distributions illustrated in Fig. 7 also demonstrate the remarkable indifference of the velocity

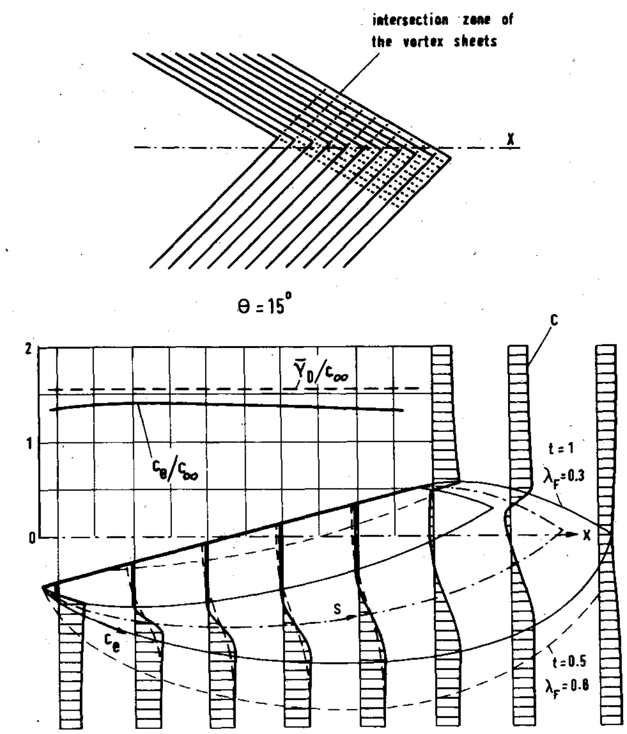

Fig. 6 Velocity distribution in the wake.

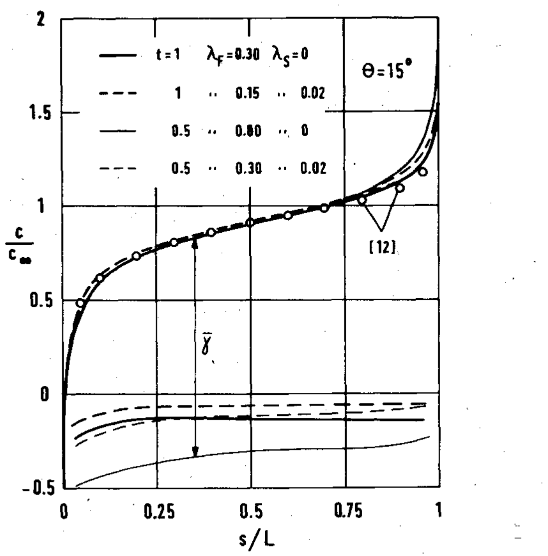

Fig. 7 Influence of shed vorticity distribution on velocity at plate surface.

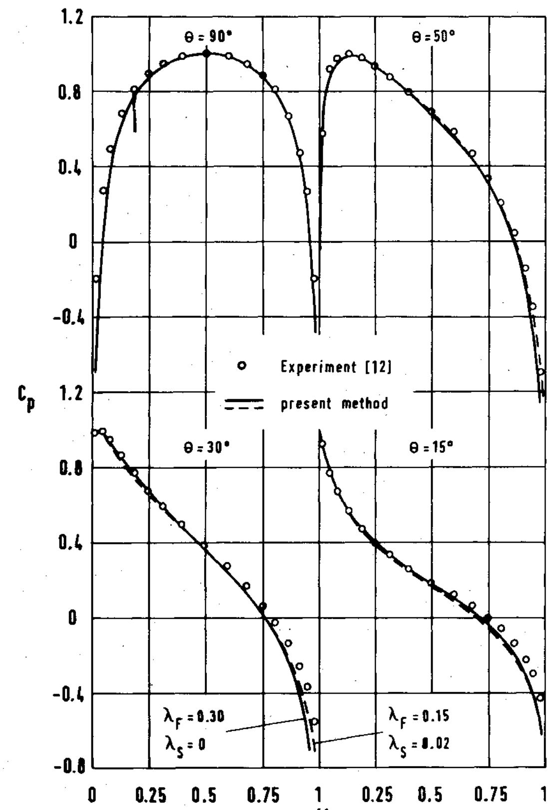

Fig. 8 Prediction accuracy for the turbulent plate flow.

at the windward side of the plate to the exact vorticity distribution downstream of the plate and its good agreement with the experiment.[12] Similar results were obtained for the other plate inclinations and are illustrated in Fig. 8. In the trailing-edge region the calculated velocity is too high at small plate inclinations, a fact that may result from the boundary layer being neglected. The computation time of these flows was 1-5 min, depending on the plate inclination.

Separated Trailing-Edge Flow

Another important application of the present method is to the flow past a thick trailing edge of an aerodynamical profile. In the following, only the case of a blunt trailing edge, with well-defined separation points, will be treated. However, the flow past a round trailing edge is not very different, since the undeterminacy about the location of the separation points affects the distance between the two vortex sheets leaving the profile to only a slight extent and therefore has little influence on the velocity field. To calculate this flow, an infinitely long, parallel-walled profile was considered, which terminates either with or without a circular arc taper (Fig. 9). The boundary condition [Eq. (18)] was formulated at discrete points of the profile contour ABDE and the centerlines BC and DC of the vortex sheets. Here it was assumed that the vortex strength is zero on the section BD and has a constant value $\pm c_\infty$ on the profile lines extending from points A and E to infinity. Again neglecting the boundary layers and choosing the distance AB as $10L$, the influence of these lines was determined analytically. The solution to the equation system thus obtained gave the vorticity distributed on segments AB and DE, the vorticity leaving the trailing edge and the shape of the free vortex sheets.

The influence of diffusion and dissipation of the vorticity on the magnitude of the shed vorticity and therefore the base pressure is illustrated in Fig. 9 for various tapers of the profile. It appears that the base pressure can be broken down into two components. The first is the pressure which comes into action in the absence of vorticity diffusion and lies, depending upon the trailing-edge taper, between the freestream pressure and the total pressure. It is therefore always an overpressure. The second component arises from the diffusion of the vorticity flowing downstream, which induces a curvature of the dividing streamline and therefore an excess velocity at the trailing edge, as illustrated in Fig. 10. The resulting "viscous" underpressure is indicated in Fig. 9 by the full lines corresponding to the parallel-walled trailing edge ($d/L = 1$). In order to compare this underpressure with the experiment, the flow around the blunt trailing-edge section measured in Ref. 13 was calculated for an incompressible fluid and a diffusion coefficient $\lambda_F = 0.33$. It will be seen in Fig. 10 that the pressure at the profile surface and on the base is in good agreement with the experiment. A second calculation with $\lambda_F = 0.15$ and $\lambda_S = 0.02$ has given practically the same result. Thus, the actual base pressure of 1.4 for the plate normal to the wind ($Re \simeq 10^6$) and of 0.6 for

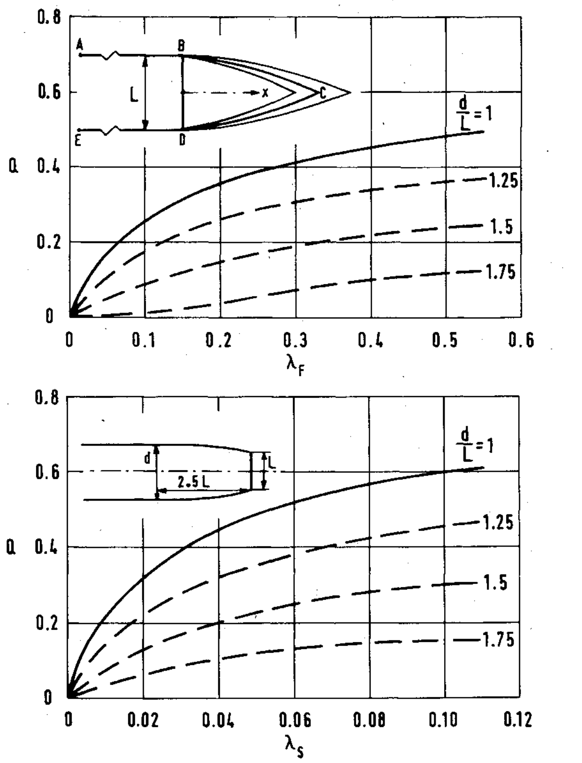

Fig. 9 Dependence of shed vorticity upon its diffusion or dissipation.

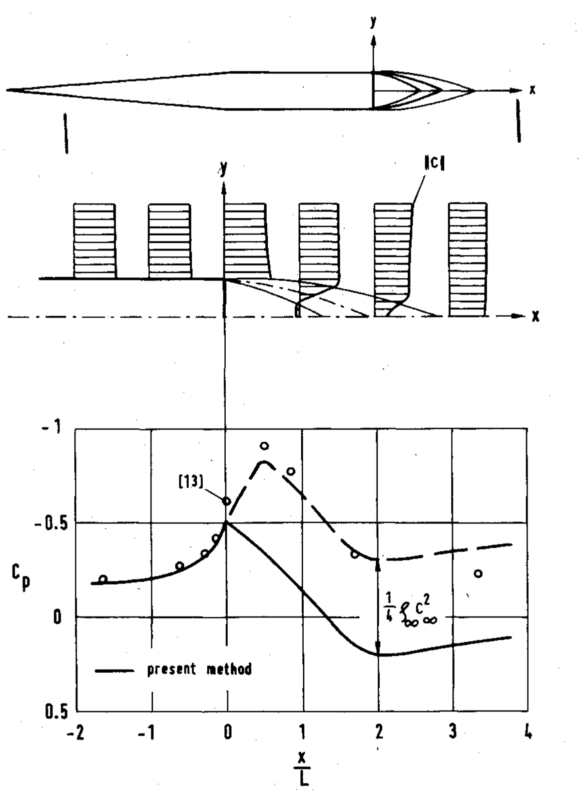

Fig. 10 Predicted pressure distribution on the afterbody surface and wake centerline.

the blunt trailing-edge section ($Re \simeq 10^6$) were obtained with the same amount of vorticity diffusion.

However, downstream of the base, the agreement between calculation and experiment is far from being satisfactory. This results from the fact that the pressure in the wake was obtained from the isentropic pressure variation in the mainstream. In fact, just downstream of the base, the wake pressure seems to fall rapidly under this calculated value, by an amount which remains constant and corresponds approximately to the dissipation of half the kinetical energy of the freestream (dotted line in Fig. 10).

Conclusion

The results presented in this study show that, for a given body shape, the extension and underpressure of the wake directly depend on the amount of diffusion and dissipation of the shed vorticity. On the other hand, the good agreement between experiment and calculations using the same vorticity diffusion for different plate inclinations and body shapes demonstrate the dominant influence of the boundary conditions on the shed vorticity and the underpressure. It confirms also the validity of a steady-state flow model for calculating separated flows having nearly constant body circulation.

The potential application of the method to profile and base flows may be evaluated from the several following considerations. By solving a mixed boundary condition problem involving vorticity diffusion, a number of assumptions concerning the strength of the shed vorticity, the location of the reattachment point, and the wake shape made by currently used methods[2-4,14] can be avoided. Therefore, the present approach may be considered as improving the solution to the kinematic problem for high Reynolds numbers. On the other hand, the assumptions on vorticity diffusion, inherent to the formulation of inverse homogeneous boundary conditions, lead to a time-consuming iteration between the velocity calculation and the boundary-layer analysis. However, this situation could be improved by introducing some viscous/inviscid interaction (e.g., Ref. 3). Finally, it should be possible to refine the simple kinetic models used here and to account, in particular, for the influence of the time-dependent fluctuations of the real flow on the local value of the diffusion and dissipation coefficients.

References

[1]Leonard, A., "Vortex Methods for Flow Simulation," *Journal of Computational Physics*, Vol. 37, Oct. 1980, pp. 289-335.

[2]Maskew, B. and Dvorak, F. A., "The Prediction of C_{max} Using a Separated Flow Model," *Journal of the American Helicopter Society*, Vol. 23, April 1978, pp. 2-8.

[3]Gilmer, B. R. and Bristow, D. R., "Analysis of Stalled Airfoils by Simultaneous Perturbations to Viscous and Inviscid Equations," *AIAA Journal*, Vol. 20, Sept. 1982, pp. 1160-1166.

[4]Geropp, D. and Grashof, J., "Berechnung von Strömungsfeldern mit Ablöseblasen bei grossen Reynoldszahlen," Deutsche Luft und Raumfahrt, Rept. DLR-FB 76-52, 1976.

[5]Gurevich, M. I., *Theory of Jets in Ideal Fluids*, Pergamon Press, New York, 1965, pp. 119-128.

[6]Ribaut, M., "A Kinematical Study of Kirchhoff-Rayleigh Flow," *Zeitschrift für Angewandte Mathematik und Physik*, Vol. 31, Jan. 1980, pp. 83-93.

[7]Ribaut, M. and Scheld, R., "A Hybrid Method for Calculating Vector Fields Subject to Inhomogeneous Boundary Conditions," *Zeitschrift für Angewandte Mathematik und Physik*, Vol. 30, May 1979, pp. 503-513.

[8]Coles, D. E., "The Law of the Wake in the Turbulent Boundary Layer," *Journal of Fluid Mechanics*, Vol. 1, Jan. 1956, pp. 191-226.

[9]Fage, A. and Johansen, F. C., "The Structure of Vortex Sheets," *Philosophical Magazine*, Ser. 7, Vol. 5, Feb. 1928, pp. 417-441.

[10]Obuchow, A. M. and Jaglom, A. M., "Die Mikrostruktur einer Turbulenten Strömung," *Statistische Theorie der Turbulenz*, Akademischer Verlag, Berlin, 1958, pp. 97-125.

[11]Helmholtz, H., "Uber Diskontinuierliche Flüssigkeitsbewegungen," *Monats-Berichte Berliner Akademie*, Vol. 23, April 1968, pp. 215-228.

[12]Fage, A. and Johansen, F. C., "On the Flow of Air Behind an Inclined Flat Plate of Finite Span," *Proceedings of the Royal Society of London*, Vol. A116, Sept. 1927, pp. 170-197.

[13]Nash, J. F., Quincey, V. G., and Callinan, J., "Experiments on Two-Dimensional Base Flow at Subsonic and Transonic Speeds," NPL Aero. Rept. 1070, 1963.

[14]Tanner, M., "Theoretical Prediction of Base Pressure for Steady Base Flow," *Progress in Aerospace Sciences*, Vol. 14, 1973, pp. 177-225.